Conformations of Chiral Molecules in Solution: Ab Initio Vibrational Absorption and Circular Dichroism Studies of 4,4a,5,6,7,8-Hexahydro-4a-methyl-2(3*H*)-naphthalenone and 3,4,8,8a-Tetrahydro-8a-methyl-1,6(2*H*,7*H*)-naphthalenedione

A. Aamouche, F. J. Devlin, and P. J. Stephens*

Contribution from the Department of Chemistry, University of Southern California, Los Angeles, California 90089-0482

Received February 11, 2000

Abstract: Studies of the vibrational unpolarized absorption and vibrational circular dichroism (VCD) spectra of the bicyclic chiral molecules: 4,4a,5,6,7,8-Hexahydro-4a-methyl-2(3*H*)-naphthalenone (**1**) and 3,4,8,8a-Tetrahydro-8a-methyl-1,6(2*H*,7*H*)naphthalenedione (**2**) are reported. Experimental spectra are compared to spectra calculated using ab initio density functional theory (DFT), hybrid functionals (B3PW91 and B3LYP), gauge-invariant atomic orbitals (GIAOs), and the 6-31G* basis set. **1** and **2** are flexible molecules. Three conformations -"trans-chair" (I), "cis-chair" (II) and "trans-boat" (III)- of **1** and **2** have been studied. Predicted relative energies are I < II < III. Comparison of predicted spectra for the three conformations to experimental mid-IR spectra in CCl_4 and CS_2 solutions unambiguously demonstrates that for both **1** and **2** conformation I is the preferred conformation in these solvents. The predicted energy differences of conformations I and II are ∼1.8 and ∼1.2 kcal/mol in **1** and **2** respectively. Weak bands in the vibrational spectra of **2** can be attributed to conformation II. Their intensities are consistent with the predicted energy difference. Bands attributable to conformation II are not definitively observed in the vibrational spectra of **1**, consistent with the greater energy difference predicted. X-ray crystallography has shown that conformation I is the conformation of **2** in the solid state; our work demonstrates that the conformation of **2** is the same in solution (in CCl_4 and CS_2) and in the crystalline solid state.

Introduction

We report studies of the chiral molecules 4,4a,5,6,7,8-Hexahydro-4a-methyl-2(3*H*)-naphthalenone, **1**, and 3,4,8,8a-Tetrahydro-8a-methyl-1,6(2*H*,7*H*)naphthalenedione (the Wieland-Miescher ketone), **2**, using ab initio vibrational spectroscopy.

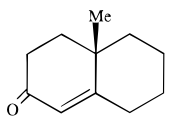

S(+)-**1**

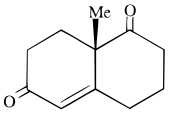

S(+)-**2**

1 and **2** are flexible molecules; we seek to establish the conformations present in solution.

Vibrational spectra sensitively reflect molecular structure. In particular, different conformations of flexible molecules exhibit distinct vibrational spectra. Accordingly, vibrational spectroscopy can be a powerful tool for conformational analysis. A variety of vibrational spectroscopies are available, including unpolarized absorption, linearly polarized Raman scattering and, for chiral molecules, circular dichroism and differential circularly polarized Raman scattering spectroscopies. Recent developments in ab initio density functional theory (DFT) have greatly enhanced the accuracy and efficiency of the ab initio prediction of the vibrational unpolarized absorption spectra of organic molecules and, in the case of chiral molecules, of their vibrational circular dichroism (VCD) spectra.[1−4] These developments include: (1) the development and implementation of analytical derivative techniques for the calculation of harmonic force fields (HFFs) and atomic polar tensors (APTs);[5] (2) the development and implementation of techniques for the calculation of atomic axial tensors (AATs) using gauge-invariant atomic orbitals (GIAOs);[1] (3) the introduction of hybrid density functionals.[6] This advance greatly facilitates the practical application of vibrational unpolarized absorption and VCD spectroscopies to conformational analysis.

We have previously reported conformational analysis of the chiral molecules 1,5-dimethyl-6,8-dioxabicyclo[3.2.1] octane (frontalin),[7] phenyloxirane,[8] 3-methyl cyclohexanone,[9] methyl lactate,[10] and dimethyl tartrate[10] using ab initio DFT, together

* To whom correspondence should be addressed: E-mail: stephens@chem1.usc.edu.

(1) Cheeseman, J. R.; Frisch, M. J.; Devlin, F. J.; Stephens, P. J. *Chem. Phys. Lett.* **1996**, *252*, 211.
(2) Stephens, P. J.; Ashvar, C. S.; Devlin, F. J.; Cheeseman, J. R.; Frisch, M. J. *Mol. Phys.* **1996**, *89*, 579.
(3) Devlin, F. J.; Stephens, P. J.; Cheeseman, J. R.; Frisch, M. J. *J. Phys. Chem.* **1997**, *101*, 6322.
(4) Devlin, F. J.; Stephens, P. J.; Cheeseman, J. R.; Frisch, M. J. *J. Phys. Chem.* **1997**, *101*, 9912.
(5) (a). Johnson, B. G.; Frisch, M. J. *Chem. Phys. Lett.* **1993**, *216*, 133. (b). Johnson, B. G.; Frisch, M. J. *J. Chem. Phys.* **1994**, *100*, 7429.
(6) Becke, A. D. *J. Chem. Phys.* **1993**, *98*, 1372, 5648.
(7) Ashvar, C. S.; Stephens, P. J.; Eggimann, T.; Wieser, H. *Tetrahedron: Asymmetry* **1998**, *9*, 1107.
(8) Ashvar, C. S.; Devlin, F. J.; Stephens, P. J. *J. Am. Chem. Soc.* **1999**, *121*, 2836.
(9) Devlin, F. J.; Stephens, P. J. *J. Am. Chem. Soc.* **1999**, *121*, 7413.
(10) Stephens, P. J.; Devlin, F. J. *Chirality* **2000**, *12*, 172; Devlin, F. J.; Stephens, P. J., to be published.

10.1021/ja000522e CCC: $19.00
Published on Web 07/14/2000

with unpolarized absorption and VCD spectroscopies. Here, we extend these studies to the two bicyclic chiral molecules, **1** and **2**, with the goal of determining their preferred conformations in solution. Predicted DFT structures for **2** are also compared to the previously reported solid-state structure, obtained by X-ray crystallography.[11]

Methods

Unpolarized absorption spectra of CCl_4 and CS_2 solutions of **1** and **2** were measured at 1 cm^{-1} resolution using a Nicolet MX1 FTIR spectrometer. Unpolarized absorption and VCD spectra of CCl_4 and CS_2 solutions were measured at 4 cm^{-1} resolution using Bomem/BioTools Chiral*IR* spectrometers. VCD scans were 1 h. Baselines for VCD spectra were obtained using racemic mixtures. In the case of **1**, where both enantiomers are available, "half-difference" and "half-sum" spectra defined as $^1/_2\{[\Delta\epsilon(1) - \Delta\epsilon(\pm)] - [\Delta\epsilon(2) - \Delta\epsilon(\pm)]\}$ and $^1/_2\{[\Delta\epsilon(1) - \Delta\epsilon(\pm)] + [\Delta\epsilon(2) - \Delta\epsilon(\pm)]\}$ (1 and 2 denote enantiomers 1 and 2) were obtained. The former provides a VCD spectrum of improved S:N ratio. The latter provides a gauge of the mirror-image symmetry of the spectra of the two enantiomers and hence of the reliability of the VCD spectrum. Deviations from mirror-image symmetry originate in both noise and polarization artifacts.

Absorption and VCD spectra were fit, assuming Lorentzian band shapes, to determine vibrational frequencies, dipole strengths, and rotational strengths using the PeakFit software [SPSS Inc., IL] as described previously.[3,4]

Equilibrium geometries and harmonic vibrational frequencies, dipole strengths, and rotational strengths were predicted using DFT. All calculations were carried out using direct analytical derivative methods via the GAUSSIAN program,[12] as described previously.[1−4,7−10] DFT calculations were carried out using the B3PW91[6,13] and B3LYP[13] functionals. The 6-31G* basis set[14] was used throughout. Atomic axial tensors (AATs)[15] were calculated using gauge-invariant atomic orbital (GIAO) basis sets.[1] Absorption and VCD spectra were obtained from calculated frequencies, dipole strengths, and rotational strengths using Lorentzian band shapes.

S(+)- and *R*(−)-**1** were obtained from Aldrich. Specified purities were 97 and 97%, respectively; specified specific rotations were $[\alpha]_D^{19} = +211.1°$ ($c = 1$, ethanol) and $[\alpha]_D^{19} = -208.3°$ ($c = 1$, ethanol), respectively. Optical purities (ee) were >95% (gc). Solutions of racemic **1** were made by mixing solutions of *S*(+)- and *R*(−)-**1**. FTIR spectra of samples of *S*(+)- and *R*(−)-**1** varied, indicating variable chemical purity. *S*(+)-**2** and (±)-**2** were obtained from Aldrich. Specified purities were 98 and 98%, respectively. The specified specific rotation of *S*(+)-**2** was $[\alpha]_D^{20} = +98°$ ($c = 1.1$, benzene). Optical purity (ee) was >99% (gc). FTIR spectra of all samples of *S*(+)- and (±)-**2** were indistinguishable.

Results

4,4a,5,6,7,8-Hexahydro-4a-methyl-2(3H)-naphthalenone, 1. Equilibrium structures of three conformations of **1** have been calculated at the B3PW91/6-31G* and B3LYP/6-31G* levels. Key structural parameters are given in Table 1, Supporting Information. The B3PW91/6-31G* structures are shown in Figure 1. In all three structures C2, C3, O1, C4, C5, C6, and C10 are approximately coplanar. The dihedral angles C2C3C4C5, O1C3C4C5, C3C4C5C6, and C3C4C5C10 deviate from their coplanar values by <10° in all structures, with the exception of C3C4C5C6 in II. In structures I and III, C1 and C11 are on opposite sides of this "enone plane". In structure II, C1 and C11 are on the same side of this plane. In structures I and II, the C5C6C7C8C9C10 ring is in a chair conformation; in III it is in a boat conformation. The relative energies of I, II, and III are given in Table 1. B3PW91/6-31G* and B3LYP/6-31G* energies are ordered: I < II < III. Thus, the "trans" conformation of C1 and C11 is more stable than the "cis" conformation, and the chair conformation of C5C6C7C8C9C10 is more stable than the boat conformation. Populations at room temperature predicted from these energies assuming a Boltzmann distribution are also given in Table 1. The populations of II and III are predicted to be 4−5 and <1% respectively.

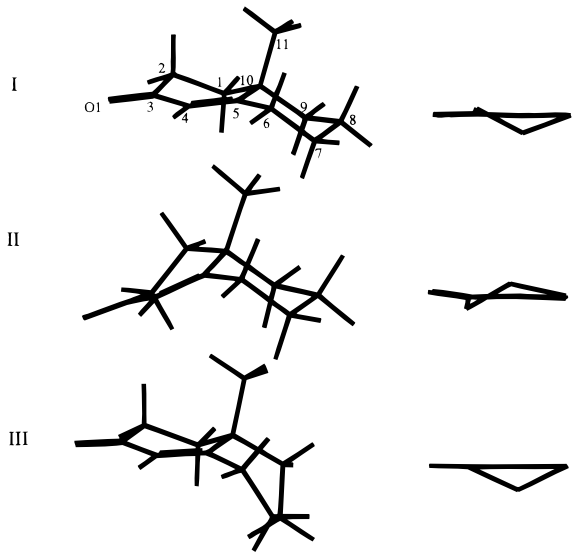

Figure 1. 4,4a,5,6,7,8-Hexahydro-4a-methyl-2(3*H*)-naphthalenone, **1**: B3PW91/6-31G* structures of conformations I, II, and III of S-**1**. The right-hand views (C4C5 toward the viewer) illustrate the conformations of the C1C2C3(O1)C4C5C10 moiety.

Table 1. Energies and Populations of Conformers I, II, and III of **1** and **2**[a]

	1						**2**					
	I		II		III		I		II		III	
	E	P	E	P	E	P	E	P	E	P	E	P
B3PW91	0	94.9	1.76	4.8	3.39	0.3	0	86.7	1.23	10.8	2.10	2.5
B3LYP	0	95.3	1.82	4.4	3.49	0.3	0	87.3	1.26	10.4	2.17	2.3

[a] Energies *E* in kcal/mol. Populations *P* calculated assuming a Boltzmann distribution and $T = 293$ K.

The unpolarized absorption spectra of **1** in CCl_4 and CS_2 are very similar. The spectrum in CCl_4 is shown in Figure 2 and in Figures 1 and 2, Supporting Information, over the range 350−1500 cm^{-1} except in the region of strong CCl_4 absorption, where the spectrum in CS_2 is shown. Harmonic vibrational frequencies and dipole strengths predicted at the B3PW91/6-31G* and B3LYP/6-31G* levels for conformation I are given in Table 2. Spectra predicted for conformations I, II, and III are compared to the experimental spectrum in Figure 2 and Figure 2, Supporting Information. For both functionals, the spectra

(11) Jones, C. R.; Kearns, D. R.; Wing, R. M. *J. Chem. Phys.* **1973**, *58*, 1370.

(12) Frisch, M. J.; Trucks, G. W.; Schlegel, H. B.; Scuseria, G. E.; Robb, M. A.; Cheeseman, J. R.; Zakrzewski, V. G.; Montgomery, J. A., Jr.; Stratmann, R. E.; Burant, J. C.; Dapprich, S.; Millam, J. M.; Daniels, A. D.; Kudin, K. N.; Strain, M. C.; Farkas, O.; Tomasi, J.; Barone, V.; Cossi, M.; Cammi, R.; Mennucci, B.; Pomelli, C.; Adamo, C.; Clifford, S.; Ochterski, J.; Petersson, G. A.; Ayala, P. Y.; Cui, Q.; Morokuma, K.; Malick, D. K.; Rabuck, A. D.; Raghavachari, K.; Foresman, J. B.; Cioslowski, J.; Ortiz, J. V.; Stefanov, B. B.; Liu, G.; Liashenko, A.; Piskorz, P.; Komaromi, I.; Gomperts, R.; Martin, R. L.; Fox, D. J.; Keith, T.; Al-Laham, M. A.; Peng, C. Y.; Nanayakkara, A.; Gonzalez, C.; Challacombe, M.; Gill, P. M. W.; Johnson, B.; Chen, W.; Wong, M. W.; Andres, J. L.; Head-Gordon, M.; Replogle, E. S.; Pople; J. A. *Gaussian 98*; Gaussian, Inc.: Pittsburgh, PA, 1998.

(13) Stephens, P. J.; Devlin, F. J.; Chabalowski, C. F.; Frisch, M. J. *J. Phys. Chem.* **1994**, *98*, 11623.

(14) Hehre, W. J.; Schleyer, P. R.; Radom, L.; Pople, J. A. *Ab initio Molecular Orbital Theory*, Wiley: New York, 1986.

(15) (a). Stephens, P. J. *J. Phys. Chem.* **1985**, *89*, 748. (b). Stephens, P. J. *J. Phys. Chem.* **1987**, *91*, 1712. (c). Stephens, P. J.; Jalkanen, K. J.; Amos, R. D.; Lazzeretti, P.; Zanasi, R. *J. Phys. Chem.* **1990**, *94*, 1811.

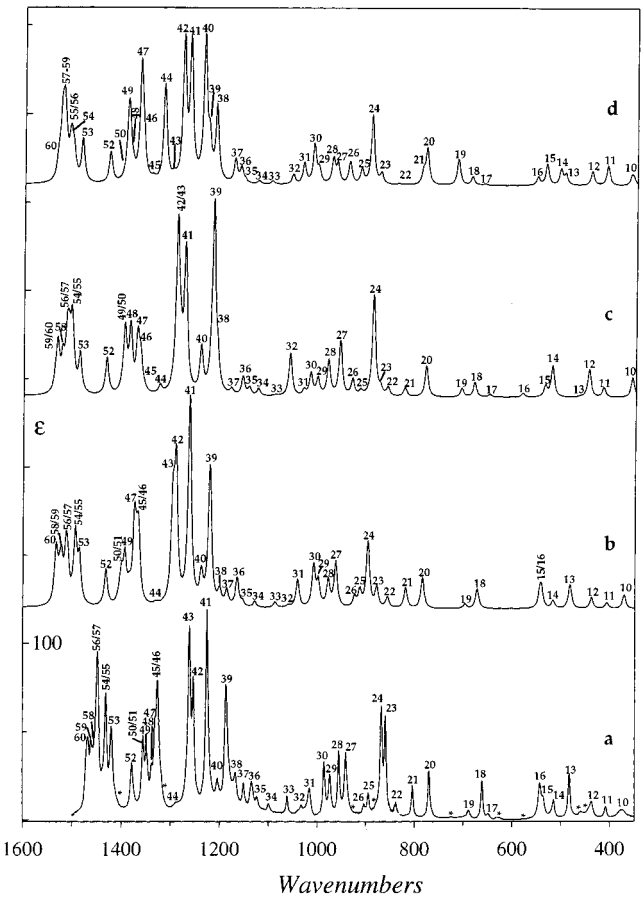

Figure 2. Calculated and experimental mid-IR absorption spectra of **1**. (a) Experimental spectrum of *S*(+)-**1** in CCl_4 (0.12 M; 830−1500 cm^{-1} and 1.04 M; 350−690 cm^{-1}) and in CS_2 (0.61 M; 690−830 cm^{-1}). (b) Conformation I spectrum. (c) Conformation II spectrum. (d) Conformation III spectrum. All calculated spectra are for B3PW91/6-31G*; Lorentzian band shapes are used ($\gamma = 4.0$ cm^{-1}). Fundamentals are numbered. In a, numbers refer to conformation I. Asterisks indicate bands not assigned as fundamentals of I.

predicted for I, II, and III are significantly different. For each structure the B3PW91 and B3LYP spectra are similar overall. The spectra of I are in better agreement with the experimental spectrum than the spectra of II and III. The experimental spectrum is therefore consistent with the theoretical prediction that structure I is the preferred conformation. Assignment of the absorption spectrum of **1**, based on the spectra predicted for I, is detailed in Figure 2a and Figure 2a, Supporting Information.

A large fraction of the fundamentals 10−60 are clearly visible in the experimental spectrum. Fundamentals 10−44, 49, 52, 53, and 60 are resolved and unambiguously assignable. Fundamentals 47 and 48 are visible as shoulders to the band at 1326 cm^{-1}, attributable to fundamentals 45 and 46. Fundamentals 50/51 are not resolved. The fundamentals 54−59 are partially resolved.

As detailed in Table 2, Figure 2a and Figure 2a, Supporting Information, nine bands are observed in the mid-IR absorption spectrum of **1** which cannot be assigned to fundamentals of conformation I. These could be due to overtone/combination bands of I, fundamentals of conformation II or impurities. Comparison of the experimental spectrum to spectra predicted for mixtures of conformations I and II leads to the conclusion that, with the possible exception of the 444 cm^{-1} band which might originate in fundamental 12 of conformation II, these bands are not attributable to conformation II. The unassigned bands are therefore attributed to either overtone/combination bands of I or to impurities. We have observed that the absorption spectra of samples of **1** vary, indicating some variation in chemical purity. The spectra in Figure 2 and Figures 1 and 2, Supporting Information are for the sample exhibiting the least impurity absorption. However, contributions from residual impurities may still be present.

Table 2. Frequencies, Dipole Strengths, and Rotational Strengths of **1**[a]

	expt.[b]			B3PW91			B3LYP		
mode[c]	ν	D	R	ν	D	R	ν	D	R
62	1680	458.2	(+)	1790	651.3	30.9	1775	636.6	29.8
	1669	389.8	(+)						
61	1619	107.6	(+)	1693	128.9	15.5	1682	119.7	14.4
60	1469	30.0	23.0	1533	23.0	11.6	1539	18.3	8.1
59	1461	6.2	2.6	1526	7.8	1.5	1533	4.9	2.2
58	1455	38.1	3.8	1522	14.9	−3.5	1528	10.7	−3.5
57				1513	18.9	−4.0	1521	13.0	−2.1
	1448	51.2	−12.6						
56				1510	12.9	1.2	1517	9.0	0.7
55				1499	0.5	0.0	1507	0.6	0.7
	1431	39.5	−2.1						
54				1494	29.9	−3.3	1503	22.4	−2.4
53	1420	31.8	4.0	1486	19.7	1.0	1494	15.5	−1.1
52	1378	24.3	−13.8	1432	16.6	−5.7	1440	12.4	−3.9
51				1405	2.7	−11.8	1409	1.6	−3.7
	1356	25.9	11.6						
50				1401	12.6	6.9	1406	12.1	−7.7
49	1348	23.1	−16.3	1394	21.4	−15.6	1392	18.3	−10.2
48	1338	10.1	−2.3	1385	5.3	6.8	1388	10.1	10.2
47	1332	15.2	27.0	1374	38.0	27.7	1378	8.0	0.3
46				1369	12.0	24.2	1371	24.7	45.0
	1326	57.0	31.1						
45				1366	29.7	4.9	1365	26.0	1.7
44	1286	7.6	−8.9	1331	1.2	−4.0	1332	1.2	−4.7
43	1262	83.0	41.7	1297	47.3	22.6	1296	17.0	13.4
42	1253	36.5	0.1	1290	67.2	15.7	1290	100.6	24.7
41	1225	87.9	−15.1	1262	107.8	−14.9	1262	111.0	−4.7
40	1205	18.6	−14.5	1238	15.1	−15.1	1237	13.1	−15.2
39	1186	72.9	−45.8	1221	74.8	−36.9	1218	95.3	−33.5
38	1168	34.0	14.2	1200	8.0	4.8	1202	12.2	4.5
37	1151	11.1	−3.2	1186	8.7	0.8	1182	9.8	−7.8
36	1134	23.8	−18.6	1165	16.3	−10.7	1162	16.3	−6.1
35	1123	9.0	5.2	1153	2.7	−0.9	1147	2.2	4.4
34	1099	10.7	3.5	1129	3.5	3.6	1129	4.2	5.7
33	1061	11.3	10.2	1087	3.5	5.6	1079	3.5	4.2
32	1033	9.3	5.2	1060	1.6	2.6	1062	1.0	0.3
31	1016	21.3	−3.3	1041	17.6	−3.4	1034	12.7	−2.8
30	986	22.9	−0.6	1008	26.7	−8.2	1005	25.4	−17.4
29	974	21.8	−6.9	998	15.8	−5.5	995	10.0	5.1
28	955	27.3	−44.3	978	17.7	−21.2	976	18.5	−20.0
27	941	32.0	−14.9	963	31.1	−25.5	964	33.6	−24.1
26	904	6.9	9.8	924	7.2	5.9	922	7.4	2.9
25	894	12.5	−5.5	913	11.8	6.5	907	4.7	−4.8
24	868	56.6	−13.3	896	48.3	−12.8	898	47.9	−1.3
23	859	43.6	10.3	878	14.7	1.0	873	7.7	0.8
22	838	13.2	−7.4	856	8.2	−6.1	850	7.0	−8.2
21[d]	804	16.6	−32.4	819	16.5	−24.7	818	11.4	−15.6
20[d]	770	27.1	12.9	784	26.0	11.8	782	26.1	10.1
19	689	7.3		697	4.4	−0.8	695	3.7	−1.3
18	661	21.8		672	19.5	−3.2	670	18.4	−8.3
17	649	3.7		658	0.1	−0.1	654	0.8	3.1
16	543	35.9		544	17.0	−2.9	546	19.3	−6.0
15	536	19.7		541	20.3	−10.8	542	16.8	−7.2
14	515	19.9		517	9.7	7.7	519	10.5	6.5
13	483	37.6		482	32.9	10.6	485	32.3	10.3
12	437	24.1		438	16.8	12.2	440	17.0	11.9
11	408	12.8		407	9.6	3.8	408	10.2	4.1
10	374	50.3		371	24.6	10.8	374	23.3	9.6

[a] Frequencies in cm^{-1}; dipole strengths in 10^{-40} esu^2 cm^2; rotational strengths in 10^{-44} esu^2 cm^2. Rotational strengths are for the *S*(+) enantiomer. Calculated parameters are for conformer I. [b] From Lorentzian fitting of CCl_4 spectra, except where indicated. We report parameters only for bands assigned to fundamentals of conformation I. Additional bands included in the fits at 444, 458, 575, 629, 726, 879, 934, 1318, 1408, 1705 cm^{-1} are attributable to non-fundamentals or impurities (see text). [c] Modes 1−9 and 63−78 are omitted. [d] From CS_2 spectra.

The VCD spectra of **1** in CCl_4 and in CS_2 are very similar. The spectrum in CCl_4 is shown in Figure 3 and Figures 3 and

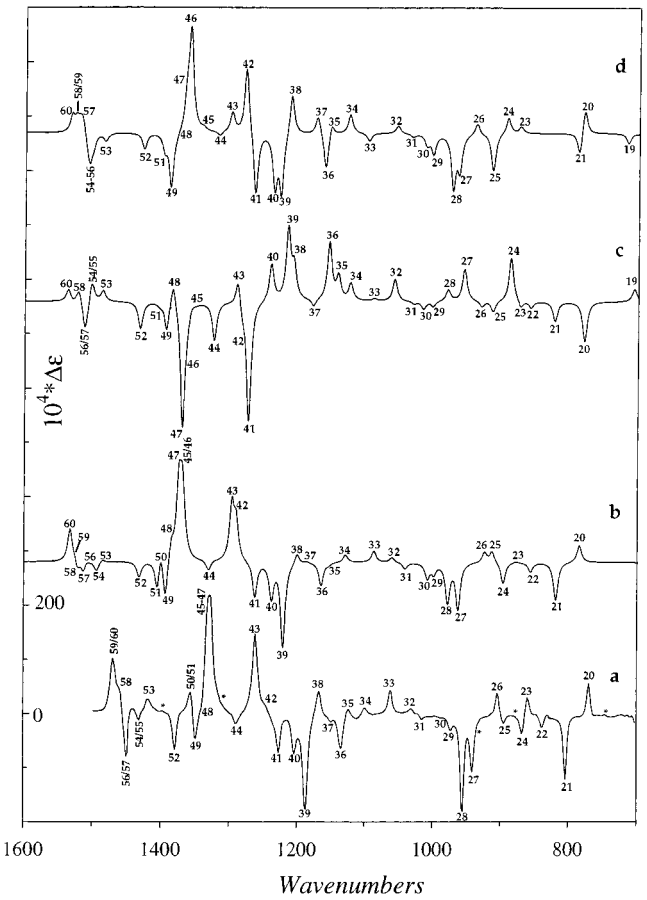

Figure 3. Calculated and experimental VCD spectra of *S*(+)-**1**. (a) Experimental spectrum: "half-difference" spectrum (see text) in CCl_4 (0.90 M; 830−1500 cm^{-1}) and in CS_2 (0.61 M; 700−830 cm^{-1}). (b) Conformation I spectrum. (c) Conformation II spectrum. (d) Conformation III spectrum. All calculated spectra are for B3PW91/6-31G*; Lorentzian band shapes are used (γ = 4.0 cm^{-1}). Fundamentals are numbered. In a, numbers refer to conformation I. Asterisks indicate bands not assigned as fundamentals of I.

4, Supporting Information, over the range 700−1500 cm^{-1} except in the region of strong CCl_4 absorption, where the spectrum of CS_2 is shown. Harmonic rotational strengths for conformation I are given in Table 2. VCD spectra predicted for conformations I, II, and III are compared to the experimental spectrum in Figure 3 and Figure 4, Supporting Information. For both functionals, the spectra predicted for I, II, and III are very different. For each structure, the B3PW91 and B3LYP spectra are similar overall. The spectra of I are in obvious agreement with the experimental spectrum; the spectra of II and III bear no resemblance to it. The VCD spectrum of **1** thus unambiguously confirms the conclusion that I is the preferred conformation.

The assignment of the VCD spectrum follows from the assignment of the absorption spectrum and is shown in Figure 3a and Figure 4a, Supporting Information. Fundamentals 20−29, 31−41, 43, 44, 49, 52, and 53 are clearly visible in the VCD spectrum; 30, 42 are not. Fundamentals 45−48, 50/51, and 54−60 are not individually resolved. The resolved fundamentals 20−22, 25−28, 31−41, 43, 49, and 52 exhibit VCD in good qualitative agreement with the B3LYP spectrum. The VCD intensities of modes 23 and 24 are much larger than predicted. The VCD intensity of mode 29 is weak, as predicted, but opposite in sign. The VCD intensities of modes 30 and 42 are much smaller than predicted. The VCD intensity of mode 53 is larger and of opposite sign than predicted. Fundamental 44 is more prominent in the VCD spectrum than in the absorption spectrum and in good agreement with prediction. The VCD of modes 45−48 is not resolved; the VCD observed is consistent with the predicted spectrum for these modes. Negative VCD is predicted for modes 50/51, opposite to the positive VCD observed. The VCD of modes 54−60 is not fully resolved; overall the observed and predicted spectra for these modes are in good agreement.

The B3PW91 spectrum exhibits significant differences from the B3LYP spectrum: the VCD of mode 24 is much larger; the VCD of modes 25 and 29 are opposite in sign; the VCD of mode 30 is much smaller; the VCD of modes 35 and 37 are opposite in sign and smaller in magnitude; the VCD of modes 49−51 differs significantly; the VCD of mode 53 is opposite in sign. In the cases of modes 24, 29, 30, 49−51 the B3PW91 spectrum is in better agreement with experiment; for modes 25, 35, and 37 the B3LYP spectrum is superior.

The C═C and C═O stretching modes, 61 and 62, are easily assigned to absorption at 1619 and 1680 cm^{-1}. The 1680 cm^{-1} C═O stretching band is split into two components, presumably due to Fermi resonance. VCD was observable in this region although with poor signal-to-noise ratio. The absorption and VCD spectra are in qualitative agreement with both B3PW91 and B3LYP predictions for conformation I. The C−H stretching absorption spectrum is complex; the C−H stretching VCD has not been measured.

The calculated frequencies, dipole strengths, and rotational strengths are compared to experimental values in Table 2 and Figure 4. Experimental parameters are obtained from Lorentzian fitting. The fits are shown in Figures 1 and 3, Supporting Information. The percentage deviation of DFT frequencies from experimental frequencies lies in the range 1−7%, increasing more-or-less monotonically with increasing frequency. B3PW91 and B3LYP frequencies are of comparable accuracy. B3PW91 dipole strengths and rotational strengths are in somewhat better agreement with experiment than B3LYP values. The accuracies of calculated frequencies, dipole strengths, and rotational strengths are comparable to those obtained in prior studies[3,4,7,8] at the 6-31G* basis set level, strongly supporting the conformational analysis and the reliability of the assignment.

3,4,8,8a-Tetrahydro-8a-methyl-1,6(2H,7H)naphthalenedione, 2. Equilibrium structures of three conformations of **2** have been calculated at the B3PW91/6-31G* and B3LYP/6-31G* levels. Key structural parameters are given in Table 1, Supporting Information. The B3PW91/6-31G* structures are shown in Figure 5. The structures I, II, and III are very similar to those of structures I, II, and III of **1**, and can likewise be described as "trans-chair", "cis-chair", and "trans-boat". The replacement of the CH_2 group at C9 by a C═O group is, as to be expected, a minor structural perturbation. For each conformation the largest changes occur in the neighborhood of C9. Thus, for conformation I, the largest bond length changes are for C8−C9 and C10−C11; the largest bond angle changes are for C8C9C10 and C9C10C11; and the largest dihedral angle changes are for C7C8C9C10, C8C9C10C1, C8C9C10C5, C8C9C10C11 and C6C5C10C9.

The relative energies of I, II, and III are given in Table 1. The ordering, as for **1**, is I < II < III. The energy differences are smaller than for **1**. As a consequence, the predicted populations of II and III, also given in Table 1, are greater than for **1**, being 10−11% for II and 2−3% for III.

The unpolarized absorption spectra of **2** in CCl_4 and CS_2 are very similar. The spectrum in CCl_4 is shown in Figure 6 and

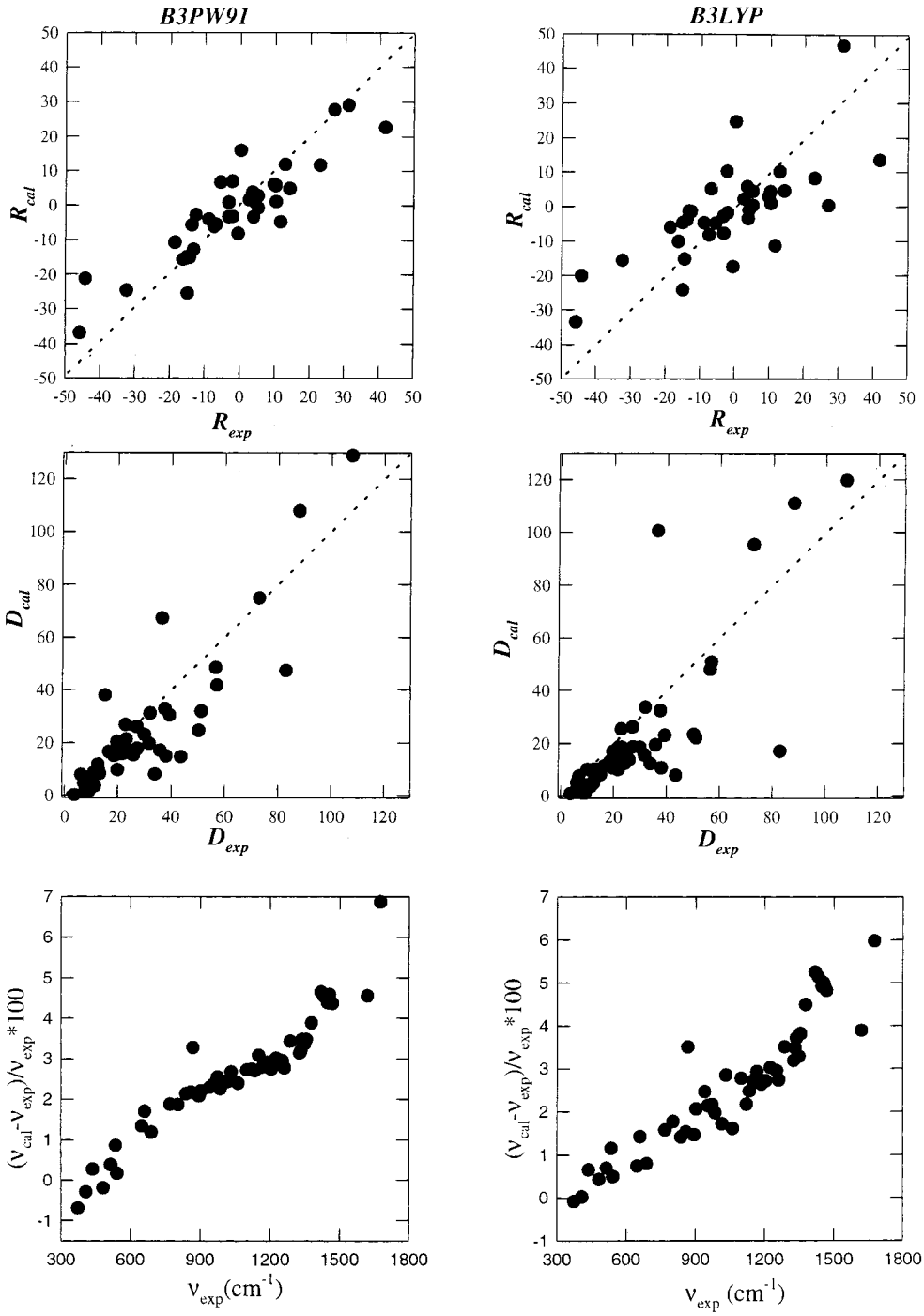

Figure 4. Comparison of calculated and experimental frequencies, dipole strengths and rotational strengths of **1**. Rotational strengths are for the *S*(+) enantiomer. The C═O stretching dipole strength (mode 62) is off-scale and is not shown. Dashed lines are of slope +1.

Figures 5 and 6, Supporting Information, over the range 360−1500 cm^{-1}, except in the region of strong CCl_4 absorption, where the CS_2 spectrum is shown. Harmonic vibrational frequencies and dipole strengths predicted at the B3PW91/6-31G* and B3LYP/6-31G* levels for conformation I are given in Table 3. Spectra predicted for conformations I, II, and III are compared to the experimental spectrum in Figure 6 and Figure 6, Supporting Information. For both functionals, the spectra predicted for I, II, and III are significantly different. For each structure the B3PW91 and B3LYP spectra are very similar overall. The spectra of I are in better agreement with the experimental spectrum than the spectra of II and III. The experimental spectrum is therefore consistent with the theoretical prediction that structure I is the preferred conformation. Assignment of the absorption spectrum of **2** based on the spectra predicted for I, is detailed in Figure 6a and Figure 6a, Supporting Information.

A large fraction of the fundamentals 10−58 are clearly visible in the experimental spectrum. Fundamentals 12−23, 25−27, 30−36, 38−45 and 51 are resolved and unambiguously assignable. Fundamentals 24 and 37 are not detectable. Fundamentals 10/11 and 28/29 are not resolved. The fundamentals 46−50 and 52−58 are partially resolved. Their assignment is more straightforward using the VCD spectrum (see below); the assignment shown in Figure 6 and Figure 6, Supporting Information is that resulting from the analysis of the VCD.

A substantial number of bands are observed in the absorption spectrum of **2** below 1100 cm^{-1} which cannot be assigned to

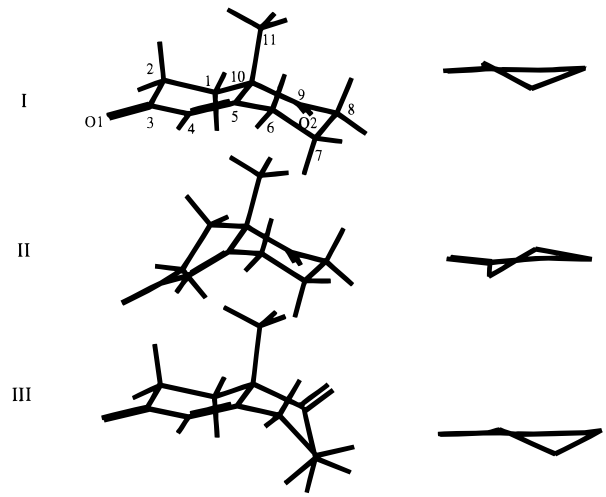

Figure 5. 3,4,8,8a-Tetrahydro-8a-methyl-1,6(2*H*,7*H*)naphthalenedione, **2**: B3PW91/6-31G* structures of conformations I, II, and III of S-**2**. The right-hand views illustrate the conformations of the C1C2C3(O1)-C4C5C10 moiety.

fundamentals of conformation I. Comparison of the experimental spectrum to spectra predicted for mixtures of conformations I and II leads to the conclusion that the majority of these bands can be assigned to fundamentals of conformation II. Specifically, fundamentals 11−15, 22, 23, 26/27, 28, and 30 of II are clearly resolved and assignable, as indicated in Figure 6a and Figure 6a, Supporting Information. The intensities of these bands, relative to those originating in fundamentals of I, are consistent with a population of II in the range 5−15%. Two bands, at 400 and 1093 cm^{-1}, are observed but not assignable to conformation II. These are attributable either to nonfundamentals of I or to impurities. Above 1100 cm^{-1}, for populations up to 20% of II, the fundamentals of II are not predicted to be resolved from those of conformation I. Consistently, no bands additional to those assigned to fundamentals of I are observed. The complete assignment of the spectrum, allowing for the contributions of both conformation I and conformation II, is detailed in Table 3.

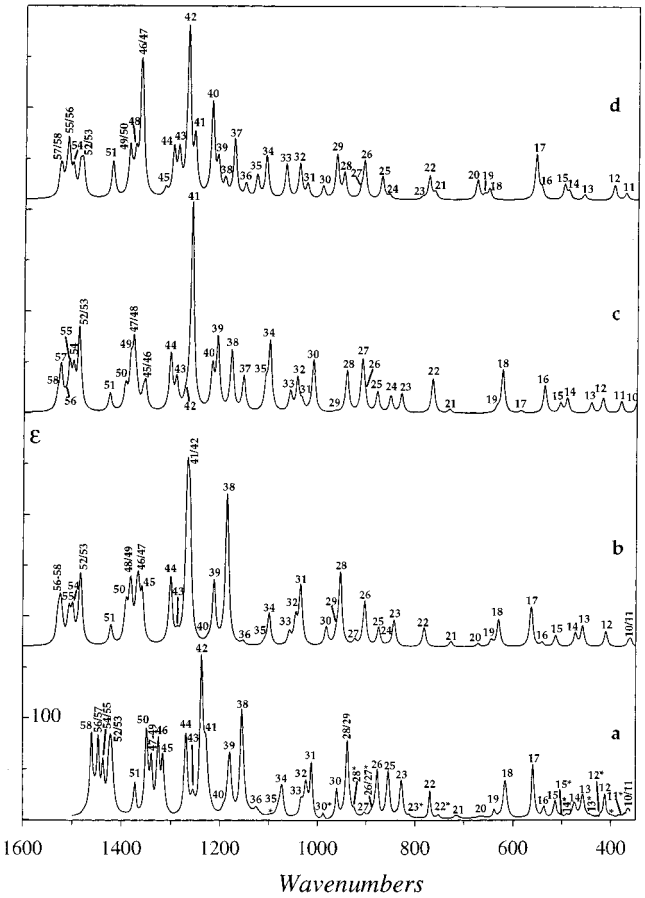

Figure 6. Calculated and experimental mid-IR absorption spectra of **2**. (a) Experimental spectrum in CCl_4 (0.50 M; 830−1500 and 0.51 M; 360−700 cm^{-1}) and in CS_2 (0.50 M; 700−830 cm^{-1}). (b) Conformation I spectrum. (c) Conformation II spectrum. (d) Conformation III spectrum. All calculated spectra are for B3PW91/6-31G*; Lorentzian band shapes are used (γ = 4.0 cm^{-1}). Fundamentals are numbered. In a, numbers refer to conformation I, except those with asterisks which refer to conformation II. Asterisks alone indicate bands not assigned as fundamentals of I or II.

The VCD spectra of **2** in CCl_4 and in CS_2 are very similar. The spectrum in CCl_4 is shown in Figure 7 and Figures 7 and 8, Supporting Information, over the range 740−1500 cm^{-1}, except in the region of strong CCl_4 absorption, where the CS_2 spectrum is shown. Harmonic rotational strengths predicted at the B3PW91/6-31G* and B3LYP/6-31G* levels for conformation I are given in Table 3. VCD spectra predicted for conformations I, II, and III are compared to the experimental spectrum in Figure 7 and Figure 8, Supporting Information. For both functionals, the spectra predicted for I, II, and III are very different. For each structure, the B3PW91 and B3LYP spectra are similar overall. The spectra of I are in obvious agreement with the experimental spectrum; the spectra of II and III are quite different. The VCD spectrum of **2** thus unambiguously confirms the conclusion that I is the preferred conformation.

The assignment of the VCD spectrum below 1260 cm^{-1} follows straightforwardly from the assignment of the absorption spectrum. Fundamentals 22, 23, 25−28, 30, and 32−43 of conformation I are clearly visible in the VCD spectrum; fundamentals 24, 29, and 31 are not. Fundamentals 22, 26/27, 28, and 30 of conformation II are also clearly visible. Above 1260 cm^{-1}, the bisignate VCD spectrum is more easily assigned than the monosignate absorption spectrum. Fundamentals 45, 46, 50, 51, 53, and 58 of conformation I are resolved; fundamentals 48/49, 54/55, and 56/57 are not resolved but observable. The VCD at the frequency of fundamental 44 of conformation I is negative, opposite in sign to that predicted. The VCD of fundamental 44 of conformation II is predicted to be much larger and negative. We therefore assign the VCD to both conformation I and II. Similarly, the negative VCD at 1338 cm^{-1} is assigned to fundamental 47 of conformation I, together with fundamentals 47 and 48 of conformation II. The assignment of the VCD spectrum is shown in Figure 7a and Figure 8a, Supporting Information. For the fundamentals 45−58, the assignment of the absorption spectrum shown in Figure 6a and Figure 6a, Supporting Information, follows from the VCD assignment. The complete assignment of the spectrum, allowing for the contributions of both conformation I and conformation II, is detailed in Table 3.

The resolved fundamentals 22, 23, 25−28, 30, 32, 34, 36, 38−43, 45, 46, 50, 51, 53, and 58 of conformation I exhibit VCD in excellent qualitative agreement with both B3PW91 and B3LYP spectra. In the case of mode 31, the B3PW91 and B3LYP VCD intensities are negative and positive respectively; the experimental VCD is positive. In the case of mode 33 the B3PW91 VCD intensity is weak and positive, as is the experimental VCD, in contrast to the B3LYP intensity which is weak and negative.The VCD of mode 35 is predicted to be weak and negative by both functionals while the observed VCD

Table 3. Frequencies, Dipole Strengths, and Rotational Strengths of **2**[a]

	expt.[b]			B3PW91			B3LYP				expt.[b]			B3PW91			B3LYP		
mode[c]	ν	D	R	ν	D	R	ν	D	R	mode[c]	ν	D	R	ν	D	R	ν	D	R
61				1826	340.7	3.7	1809	332.9	5.5	35				1109	3.7	−0.7	1109	3.7	−0.6
	1718	488.0	14.0								1080	5.1	3.9						
61*				**1825**	**353.8**	**29.3**				**35***				**1109**	**25.7**	**2.0**			
60*	1686	466.5	61.0	**1796**	**628.4**	**12.4**				**34***				**1101**	**69.6**	**2.4**			
	1677	238.4	6.0								1073	34.4	26.0						
60	1671	212.4	27.0	1793	648.7	45.3	1777	632.5	42.3	34				1100	33.5	31.3	1097	46.4	32.3
59*				**1694**	**131.8**	**−55.9**				**33***				**1059**	**20.9**	**−7.5**			
	1623	125.2	−12.0								1034	14.0	8.6						
59				1693	154.8	−12.3	1683	143.3	−12.5	33				1058	13.2	6.5	1056	1.5	−5.3
58*				**1532**	**8.8**	**−9.2**				32				1046	27.9	−39.0	1039	30.5	−31.7
	1460	60.8	17.2								1024	45.5	−59.2						
58				1529	17.9	6.3	1534	14.3	5.1	**32***				**1044**	**35.9**	**−11.1**			
57*				**1525**	**31.5**	**15.9**				31				1036	64.5	−3.7	1030	60.8	2.1
57	1447	46.6	−1.8	1524	24.8	3.6	1530	18.0	3.4		1013	40.1	7.0						
56				1521	8.6	−3.4	1527	6.5	−3.1	**31***				**1035**	**9.5**	**−11.9**			
56*				**1516**	**5.5**	**−0.3**				**30***	**989**	**1.6**	**−11.6**	**1012**	**59.0**	**−30.2**			
55*				**1508**	**30.8**	**−10.2**				30	961	23.5	−48.3	983	21.0	−20.6	981	26.7	−25.7
55	1437	23.3	9.8	1507	22.8	1.6	1515	17.2	1.2	**29***				**966**	**1.2**	**2.1**			
54*				**1500**	**25.5**	**17.2**					943	5.1	0.0						
54				1499	23.5	2.5	1507	18.1	2.1	29				962	10.3	−7.1	960	17.0	16.7
53*				**1489**	**35.8**	**−3.4**				28	939	87.0	−125.6	954	86.9	−85.3	955	77.5	−100.1
52*	1423	57.3	−10.9	**1488**	**27.2**	**−1.4**				**28***	**925**	**8.0**	**9.9**	**943**	**50.8**	**−26.5**			
53				1484	32.4	−15.1	1493	25.4	−12.5	27	904	5.1	3.0	924	6.3	−0.3	916	4.5	−4.5
52	1420	41.5	5.3	1482	24.6	3.5	1491	18.8	1.8	**27***				**911**	**61.1**	**35.5**			
51*				**1426**	**14.7**	**−1.6**					**884**	**20.2**	**−0.2**						
	1373	22.2	6.8							**26***				**907**	**12.9**	**−9.5**			
51				1422	15.6	6.9	1430	9.5	5.2	26	878	44.0	27.9	904	56.8	12.6	904	52.0	13.6
50*				**1395**	**18.1**	**−6.2**				**25***				**880**	**26.3**	**−10.4**			
	1349	63.6	−11.2								855	60.1	−39.5						
50				1391	28.7	−29.7	1394	9.9	−18.1	25				875	24.4	−17.7	875	16.9	−11.0
49*				**1384**	**33.6**	**1.6**				24				858	1.8	−0.4	854	2.3	1.4
49	1340	18.6	9.0	1383	25.2	6.8	1387	35.8	−13.6	**24***				**853**	**22.3**	**0.3**			
48				1381	26.5	9.5	1382	17.0	19.9	23	829	50.1	26.9	844	34.9	10.3	838	30.8	8.7
48*				**1378**	**49.3**	**−52.7**				**23***[d]	**812**	**5.1**	**0.0**	**831**	**26.8**	**6.9**			
47*				**1372**	**10.9**	**−40.6**				22[d]	770	26.3	33.0	782	27.7	22.4	780	25.7	18.8
	1338	15.6	−18.5							**22***[d]	**753**	**6.2**	**−2.2**	**767**	**51.1**	**−17.4**			
47				1370	23.7	−17.7	1369	5.3	−17.5	**21***[d]				**732**	**6.4**	**13.4**			
46	1325	54.5	43.0	1366	36.6	52.2	1367	46.5	45.6		715	12.9							
45				1359	37.8	34.0	1360	31.2	25.4	21[d]				727	8.3	10.4	724	6.6	9.5
46*	1316	43.5	55.4	**1359**	**9.5**	**6.8**				**20***				**679**	**0.2**	**3.1**			
45*				**1354**	**21.4**	**25.4**					666	10.8							
44*				**1303**	**48.4**	**−22.3**				20				672	5.2	5.3	669	5.3	4.2
	1269	70.8	−3.7							19	638	12.5		645	11.5	−3.8	640	19.0	−8.3
44				1301	57.4	0.1	1300	54.5	3.6	**19***				**635**	**7.8**	**14.6**			
43*				**1291**	**24.6**	**58.6**				18	616	82.3		630	48.3	−38.5	628	41.8	−37.2
	1255	12.3	28.4							**18***				**624**	**79.3**	**−26.7**			
43				1287	5.6	23.3	1287	4.4	16.3	**17***				**587**	**4.9**	**9.1**			
42*				**1272**	**5.9**	**−19.0**				17	559	89.1		563	81.2	−3.1	562	82.5	−6.6
	1238	108.4	−45.6							16				541	7.9	−4.7	542	8.5	−0.7
42				1268	128.4	−37.0	1266	215.6	−24.4		537	24.5							
41				1262	99.5	17.9	1260	24.9	17.4	**16***				**538**	**59.4**	**9.4**			
	1229	88.6	18.9							15	514	34.5		514	25.5	−20.2	515	25.4	−17.3
41*				**1260**	**188.4**	**56.4**				**15***	**503**	**9.6**		**506**	**21.8**	**24.9**			
40	1192	4.7	−12.5	1225	2.3	−0.8	1224	4.2	−5.8	**14***	**490**	**4.3**		**492**	**34.3**	**−26.3**			
40*				**1218**	**37.9**	**1.0**				14	475	44.2		473	31.8	43.3	475	29.2	39.6
39	1180	69.0	−15.9	1213	58.3	−12.2	1212	79.7	−12.2	13	458	63.1		459	50.5	34.7	459	53.8	35.0
39*				**1207**	**66.5**	**69.1**				**13***	**441**	**12.1**		**443**	**27.0**	**28.1**			
38				1186	144.9	−81.5	1180	130.9	−67.4	**12***	**421**	**5.0**		**419**	**41.6**	**5.6**			
	1155	106.4	−82.2							12	413	50.9		411	42.2	32.2	412	40.0	29.5
38*				**1179**	**57.9**	**−47.2**				**11***	**382**	**14.3**		**381**	**35.8**	**−5.1**			
37	1143	4.9	−9.1	1165	0.4	−0.8	1167	2.6	6.1	11				364	13.6	−3.9	366	15.7	−5.2
37*				**1154**	**34.0**	**35.6**					365	50.3							
36	1125	17.8	−15.7	1153	3.5	−3.6	1144	4.3	−2.8	10				360	21.2	1.0	360	20.0	1.7
36*				**1149**	**0.9**	**0.8**													

[a] Frequencies in cm^{-1}; dipole strengths in 10^{-40} esu^2 cm^2; rotational strengths in 10^{-44} esu^2 cm^2. Rotational strengths are for the $S(+)$ enantiomer. [b] From Lorentzian fitting of CCl_4 spectra, except where indicated. Other bands included in the fits at 400 and 1093 cm^{-1} are attributable either to non-fundamentals of conformation I or to impurities. [c] Numbers without and with asterisks refer to conformers I and II, respectively. Modes 1−9 and 62−75 are omitted. [d] From CS_2 spectra.

is weak but positive. The observed negative VCD of mode 37 is also in poor agreement with both B3PW91 and B3LYP predictions. The combined VCD of the overlapping modes 48/49 and 54/55 is in agreement with the predicted spectra. Fundamentals 22, 26/27, 28, and 30 of conformation II exhibit VCD whose signs are in agreement with both B3PW91 and B3LYP calculations.

The C═C and C═O stretching modes, 59−61, are easily assigned to absorption at 1623, 1686, and 1718 cm^{-1}. The 1686 cm^{-1} C═O stretching band is split, presumably due to Fermi

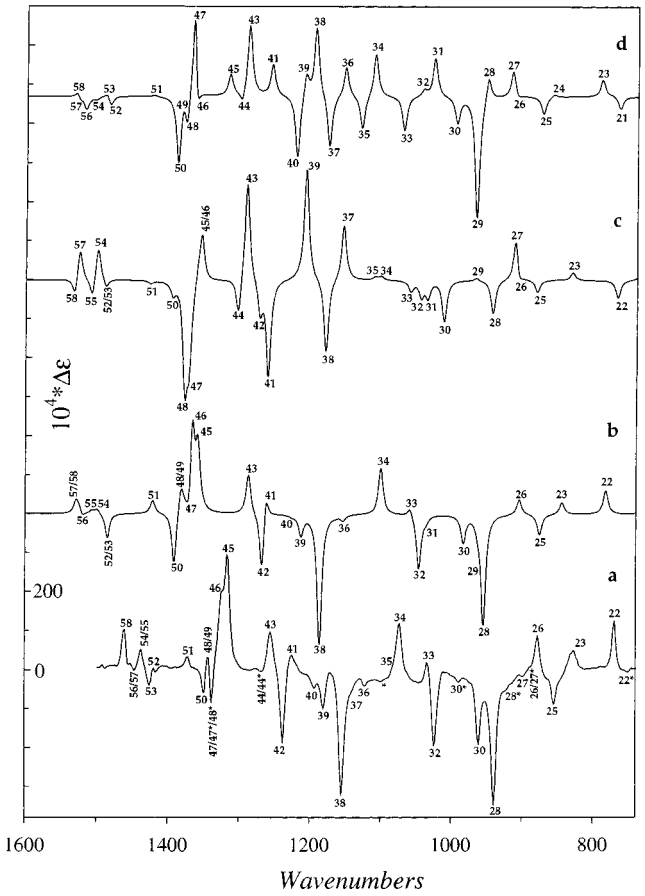

Figure 7. Calculated and experimental VCD spectra of *S*(+)-**2**. (a) Experimental spectrum: $[\Delta\epsilon(+) - \Delta\epsilon(\pm)]$ in CCl_4 (0.50M; 820−1500 cm^{-1}) and in CS_2 (0.50 M; 740−820 cm^{-1}). (b) Conformation I spectrum. (c) Conformation II spectrum. (d) Conformation III spectrum. All calculated spectra are for B3PW91/6-31G*; Lorentzian band shapes are used ($\gamma = 4.0$ cm^{-1}). Fundamentals are numbered. In a numbers refer to conformation I, except those with asterisks which refer to conformation II. Asterisks alone indicate bands not assigned as fundamentals of I or II.

resonance. VCD was clearly observable, although with poor signal-to-noise ratio. The absorption and VCD spectra are in excellent qualitative agreement with both B3PW91 and B3LYP predictions for conformation I. The C−H stretching absorption spectrum is complex; the C−H stretching VCD has not been measured.

The calculated frequencies, dipole strengths, and rotational strengths are compared to experimental values in Table 3 and Figure 8. Experimental parameters are obtained from Lorentzian fitting. The fits are shown in Figures 5 and 7, Supporting Information. In comparing B3PW91/6-31G* and experimental dipole and rotational strengths, two choices have been made: (1) the contributions of conformation II have been ignored; (2) the contributions of conformation II have been included, assuming the populations of I and II to be 90 and 10%, respectively. The agreement with experimental dipole and rotational strengths is not significantly different when the contributions of conformation II are included. Thus, comparison of calculated and experimental dipole and rotational strengths does not permit the percentage population of conformation II to be quantitated. In comparing B3LYP/6-31G* and experimental dipole and rotational strengths, the contributions of conformations II have been ignored. The accuracies of the calculated frequencies, dipole strengths, and rotational strengths are comparable to those for **1** and again support the conformational analysis and the reliability of the assignment for **2**.

Discussion

Using mid-IR vibrational unpolarized absorption and VCD spectra, we have shown that the predominant conformations of **1** and **2** in CCl_4 and CS_2 solutions are the "trans-chair" conformations, I. In the case of **2**, but not of **1**, we have also found clear evidence of a small but significant population of the "cis-chair" conformation II. B3PW91/6-31G* and B3LYP/6-31G* single molecule calculations predict that I is the conformation of lowest energy in both **1** and **2**, in agreement with our experimental results. They also predict that the energy difference between I and II is smaller in **2**, consistent with the observed greater population of II in **2**. The intensities of bands in the absorption and VCD spectra of **2** assignable to II are consistent with the predicted energy difference of ∼1.2 kcal/mol. This implies that (i) the predicted conformational energy difference is reliable and (ii) the contributions of solvation and of entropy to the conformational free energy difference in solution are not large. The nonpolar solvents CCl_4 and CS_2 are relatively innocuous; it is of course possible that solvation effects on the conformational equilibrium will be more significant in the case of other, more strongly perturbing solvents. Further work (such as temperature-dependent vibrational spectroscopy) is required to establish quantitatively the energy difference of conformations I and II in **1** and **2** in a range of solvents.

We are not aware of prior, detailed experimental studies of the conformations of **1** and **2** in solution. Crystalline racemic **2** has been studied by X-ray diffraction.[11] The conformation was found to be "trans-chair". It follows that, in the case of **2**, the conformation crystallizing from solution is the lowest-energy conformation in solution. Predicted bond lengths, bond angles, and dihedral angles for conformation I are compared to experimental values in Table 1, Supporting Information, and Figure 9, Supporting Information. The agreement is excellent. Mean absolute deviations between calculated and experimental parameters are: bond lengths, 0.008 and 0.009 Å; bond angles, 0.8/0.7°; and dihedral angles, 1.7 and 2.0° for B3PW91/6-31G* and B3LYP/6-31G*, respectively.

The change in the energy difference of conformations I and II as a result of the substitution of C═O for CH_2 at C9 is substantial. It was recognized in studies of optical rotatory dispersion (ORD) of molecules (predominantly steroids) containing a 1,3-cyclohexenone ring that the conformation of this ring is sensitive to variations in the adjacent ring(s).[16] Our results for **1** and **2** are consistent with this finding and further suggest that other substitutions in the cyclohexane ring of **1** may not only lead to larger changes in the energy difference of I and II but even cause conformation II to become the more stable. Studies of a wider range of derivatives of **1** to explore this possibility would be of interest.

The absolute configuration of **1** was first established by synthesis.[17] The absolute configuration of **2** was also first established by synthesis[18] and subsequently confirmed by electronic CD studies of a derivative.[19] Our studies provide further confirmation of the *S*(+)/*R*(−) absolute configurations of **1** and **2**.

Two recent developments have, together, greatly enhanced the practicality of vibrational spectroscopy as a tool for

(16) Djerassi, C.; Riniker, R.; Riniker, B. *J. Am. Chem. Soc.* **1956**, *78*, 6377.
(17) Djerassi, C.; Marshall, D. *J. Am. Chem. Soc.* **1958**, *80*, 3986.
(18) Prelog, V.; Azklin, W. *Helv. Chem. Acta* **1956**, *39*, 748.
(19) Harada, N.; Sugioka, T.; Uda, H.; Kuriki, T. *Synthesis* **1990**, 53.

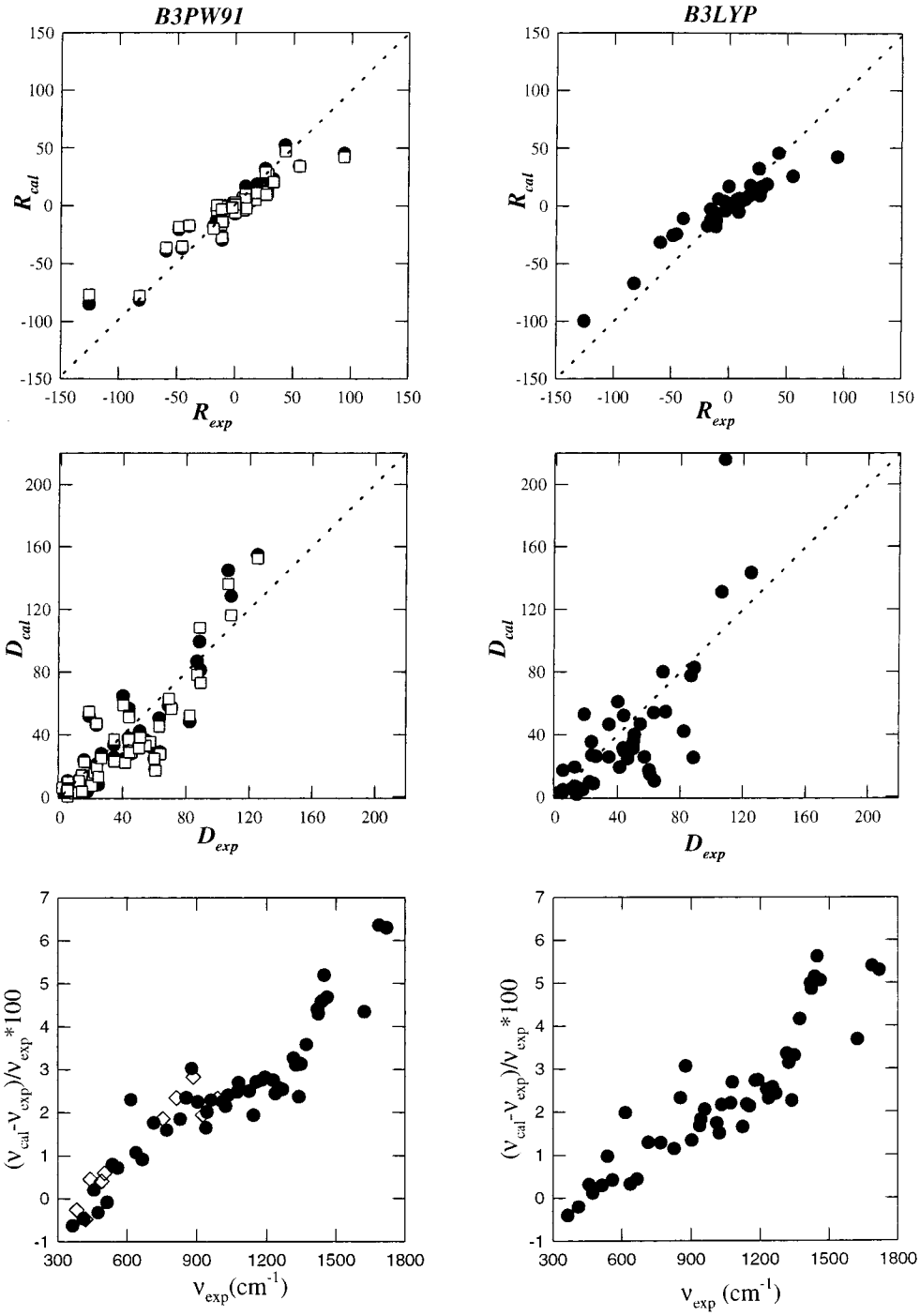

Figure 8. Comparison of calculated and experimental frequencies, dipole strengths, and rotational strengths of **2**. Rotational strengths are for the *S*(+) enantiomer. In the case of frequencies, (◇) indicates modes assigned exclusively to conformation II; for bands assigned to modes of both conformation I and conformation II, the calculated frequency for conformation I is used. In the case of dipole and rotational strengths, either contributions of conformation II are ignored (●) or included (□); in the latter case, populations of conformations I and II are assumed to be 90% and 10% respectively. The C═O stretching dipole strengths are off-scale and are not shown. Dashed lines are of slope +1.

conformational analysis. First, the development of commercial instrumentation for the measurement of VCD now permits the routine use of VCD spectra in addition to unpolarized absorption spectra. As our studies of **1** and **2** demonstrate yet again, VCD spectra are substantially more sensitive to molecular conformation than are absorption spectra. Consequently, the use of absorption spectra and VCD spectra together greatly enhances the power of vibrational spectroscopy in conformational analysis. Second, progress in the application of DFT to the calculation of harmonic vibrational frequencies, dipole strengths, and rotational strengths now permits the prediction of absorption and VCD spectra with much higher accuracy and efficiency than previously practicable. The development of hybrid functionals such as B3PW91 and B3LYP[6,13] has significantly increased the accuracy of DFT predictions.[20] The implementation of analytical derivative methods using perturbation-dependent basis sets has greatly increased both the accuracy and the efficiency of DFT predictions.[1,5] In particular, the imple-

(20) Frisch, M. J.; Trucks, G. W.; Cheeseman, J. R. In *Recent Developments and Applications of Modern Density Functional Theory*; Seminario, J. M., Ed.; *Theoretical and Computational Chemistry*, Vol. 4, Elsevier: 1996; pp 679−707.

mentation of analytical derivative methods for calculating atomic axial tensors (AATs) using gauge-invariant atomic orbitals (GIAOs) has brought the calculation of AATs to the same level of accuracy (at a given basis set level) as the calculation of APTs.[1] Consequently, DFT dipole and rotational strengths can now be calculated with equal accuracy. Studies of a number of rigid molecules have documented quantitatively the reliability of the DFT methodology in predicting absorption and VCD spectra.[1−4] Subsequently, applications to conformational analysis have been carried out for 1,5-dimethyl-6,8-dioxabicyclo [3.2.1] octane,[7] phenyloxirane,[8] 3-methylcyclohexanone,[9] methyl lactate,[10] and dimethyl tartrate.[10] The studies reported here provide further examples of the efficacy of the methodology.

At the present time, DFT calculations are carried out at the harmonic level of approximation and neglecting solvent effects. In the mid-IR spectral region, the harmonic approximation is a very good approximation, as shown by the excellent agreement between predicted harmonic spectra and experimental spectra and by the smallness of the number of observed bands which cannot be assigned to fundamental transitions. In the hydrogenic stretching region, Fermi resonance is much more important; without the inclusion of anharmonicity predictions are much less reliable. While solvent effects on VCD spectra have been very little studied experimentally, it is very likely that for specific combinations of molecules and solvents, they will be of importance. The extension of the current DFT methodology to include anharmonicity and solvent effects is clearly important to enhance its accuracy and, therefore, practical utility.[21]

Acknowledgment. NIH (GM051972-04) and NSF (CHE-9902832) grants to P.J.S. and a postdoctoral fellowship from Elf Aquitaine/Sanofi to A.A. are gratefully acknowledged.

Supporting Information Available: Table and Figures (PDF). This material is available free of charge via the Internet at http://pubs.acs.org.

JA000522E

(21) It should be noted that: (i) A formal theory of VCD intensities including anharmonicity has been developed and implemented using HF/SCF and MP2 methods: Bak, K. L.; Bludsky, O.; Jørgensen, P. *J. Chem. Phys.* **1995**, *103*, 10548. (ii) Very recently, the polarized continuum model (PCM) for solvent effects has been coupled to the ab initio HF/SCF calculation of harmonic rotational strengths: Tomasi, J.; Cammi, R.; Mennucci, B. *Int. J. Quantum Chem.* **1999**, *75*, 783; Mennucci, B.; Cammi, R.; Tomasi, J. *Int. J. Quantum Chem.* **1999**, *75*, 767.